symmetry

MDPI

Article

Reheating Constraints and the H_0 Tension in Quintessential Inflation

Jaume de Haro [1,*] and Supriya Pan [2,3]

[1] Departament de Matemàtiques, Universitat Politècnica de Catalunya, Diagonal 647, 08028 Barcelona, Spain
[2] Department of Mathematics, Presidency University, 86/1 College Street, Kolkata 700073, India; supriya.maths@presiuniv.ac.in
[3] Institute of Systems Science, Durban University of Technology, P.O. Box 1334, Durban 4000, South Africa
* Correspondence: jaime.haro@upc.edu

Abstract: In this work, we focus on two important aspects of modern cosmology: reheating and Hubble constant tension within the framework of a unified cosmic theory, namely the quintessential inflation connecting the early inflationary era and late-time cosmic acceleration. In the context of reheating, we use instant preheating and gravitational reheating, two viable reheating mechanisms when the evolution of the universe is not affected by an oscillating regime. After obtaining the reheating temperature, we analyze the number of e-folds and establish its relationship with the reheating temperature. This allows us to connect, for different quintessential inflation models (in particular for models coming from super-symmetric theories such as α-attractors), the reheating temperature with the spectral index of scalar perturbations, thereby enabling us to constrain its values. In the second part of this article, we explore various alternatives to address the H_0 tension. From our perspective, this tension suggests that the simple Λ-Cold Dark Matter model, used as the baseline by the Planck team, needs to be refined in order to reconcile its results with the late-time measurements of the Hubble constant. Initially, we establish that quintessential inflation alone cannot mitigate the Hubble tension by solely deviating from the concordance model at low redshifts. The introduction of a phantom fluid, capable of increasing the Hubble rate at the present time, becomes a crucial element in alleviating the Hubble tension, resulting in a deviation from the Λ-Cold Dark Matter model only at low redshifts. On a different note, by utilizing quintessential inflation as a source of early dark energy, thereby diminishing the physical size of the sound horizon close to the baryon–photon decoupling redshift, we observe a reduction in the Hubble tension. This alternative avenue, which has the same effect of a cosmological constant changing its scale close to the recombination, sheds light on the nuanced interplay between the quintessential inflation and the Hubble tension, offering a distinct perspective on addressing this cosmological challenge.

Keywords: quintessential inflation; reheating temperature; H_0 tension

Citation: de Haro, J.; Pan, S. Reheating Constraints and the H_0 Tension in Quintessential Inflation. *Symmetry* **2024**, *16*, 1434. https://doi.org/10.3390/sym16111434

Academic Editor: Branko Dragovich

Received: 26 August 2024
Revised: 5 October 2024
Accepted: 21 October 2024
Published: 28 October 2024

1. Introduction

Inflation and late-time cosmic acceleration are two significant eras of modern cosmology that created enormous interest and debates in the scientific community. Inflation—a rapid accelerating phase of the universe [1,2]—is a theory for the early universe that was proposed to solve a number of limitations of the hot big bang cosmology. Usually a scalar field with slowly rolling potential can drive this accelerating phase quite smoothly, and this motivated the early universe community to investigate various scalar field models with similar features [3–28] (also see [29–32]). According to the cosmic microwave background observations from various surveys [33–44], this proposal is one of the leading theories for describing the early universe. On the other hand, late-time cosmic acceleration was discovered at the end of the nineties of the past century through the observations from Type Ia supernovae [45,46]. The discovery of the accelerated expansion of the universe

gave a massive jerk on the understanding of the dynamical evolution of the universe and introduced the concept of dark energy or gravity modifications. One of the possible DE candidates is the quintessence [47–49], a canonical scalar field that was proposed as a possible alternative to the cosmological constant. One can realize that both the inflation and late-time cosmic acceleration can be described in terms of the scalar field models, but indeed both eras have different energy scales. Although the origin of these kinds of scalar fields follows a phenomenological route (see [50–52] to find several attempts to physically explain their appearance), this motivated us to introduce a new and appealing cosmological theory, known as quintessential inflation.

Quintessential inflation, a concept elaborated in [53], is a theoretical framework that unifies the early and late-time accelerated expansions of the universe, proposing a single scalar field responsible for both inflation and dark energy. This approach addresses key cosmological puzzles by merging two distinct eras of cosmic acceleration into one coherent model. At early times, the inflation field drives rapid inflation, which solves the horizon, flatness, and other problems while generating primordial density perturbations. Post-inflation, that is, after reheating and the radiation and matter domination phases, the field transits to a slow-roll regime, acting as quintessence, which explains the observed late-time acceleration. The evolution of this scalar field is governed by a potential that allows for a transition between these phases, avoiding the need for separate inflation and dark energy mechanisms. Quintessential inflation models are evaluated against observational data, such as cosmic microwave background (CMB) measurements and large-scale structure surveys, to constrain the potential forms and field dynamics, ensuring consistency with the standard cosmological model. We refer to an incomplete list of works in this direction [54–97].

After the inflation, a reheating mechanism becomes essential [98–100], because following the reheating of the universe, it transits from its cold inflationary state to a hot phase required to match with the standard Big Bang cosmology. Without reheating, we would have a universe without any matter, and this goes against the observational evidence that we have traced out so far. In our work, in the context of quintessential inflation, we review two mechanisms to reheat the universe after inflation, namely, instant preheating [101] and gravitational reheating via particle production [102–104]. And dealing with supersymmetric gravity theories such as α-attractors in quintessential inflation [105], we relate the reheating temperature with the observable parameters of the power spectrum, namely the spectral index and the ratio of tensor to scalar perturbations, showing how the reheating temperature, whose value ranges between 1 MeV and 10^9 GeV in order to guarantee the success of Big Bang Nucleosynthesis (BBN) and overpass the gravitino problem [106,107], constraint these parameters.

Now, during the second phase of quintessential inflation, that means in the era of late-time cosmic acceleration, observational data from various astronomical missions is pointing towards a discrepancy in several key cosmological parameters. One of the intriguing cosmic conundrums arises from a notable disparity between two independent measurements of the present value of the Hubble rate, denoted as H_0, which represents the current rate of cosmic expansion. More precisely, observations from the cosmic microwave background (CMB) within the ΛCDM model, utilizing the precise measurements from missions such as the Planck satellite, yield a Hubble constant value $H_0 = 67.4 \pm 0.5$ km s^{-1}Mpc^{-1} [108]. However, the late-time measurements of H_0 using the cosmic distance ladder, such as the SH0ES (Supernovae and H_0 for the Equation of State (EoS) of dark energy) team, where the Type Ia supernovae are calibrated with Cepheids, lead to $H_0 = 73.04 \pm 1.04$ km s^{-1} Mpc^{-1} [109]. These two measurements exhibit a significant tension at the level of $\sim 5\sigma$, posing a challenge to the standard cosmological paradigm and consequently hints at potential shortcomings or missing elements in the ΛCDM model. Although there is no doubt that ΛCDM cosmology has been quite successful in explaining a large number of astronomical surveys, this significant tension in H_0 argues that most probably ΛCDM is an approximate version of a more realistic theory that is under the microscope. This tension propels cosmologists to explore alternative models, extensions, or modifications that could provide a more

accurate and coherent description of the universe's expansion history. Various avenues have been explored in the literature, including the introduction of new physics, modifications to the nature of dark energy, or reconsideration of fundamental cosmological assumptions [110–112]. However, based on the existing literature, the final answer is yet to be revealed.

In the present article, within the framework of quintessential inflation, we delve into two alternative modifications of the concordance model. Firstly, we explore the deviation of the concordance model at low redshifts. In this scenario, quintessential inflation alone, without the presence of other components, proves insufficient to reconcile the Hubble tension. However, when combined with quintessential inflation, the introduction of a phantom fluid, altering the dynamics specifically at redshifts $z \lesssim 2$, emerges as a solution. This modification effectively increases the value of the Hubble rate at the present epoch, offering a means to alleviate the tension observed in the Hubble constant measurements. In the second case, we investigate the injection of dark energy, commonly referred to as early dark energy (EDE). The conceptual foundation involves presenting a potential that, akin to standard quintessential inflation, undergoes a phase transition during the early universe from inflation to kination. During this phase, the potential is nearly flat with a very small scale, mimicking characteristics of a cosmological constant. However, to imbue quintessential inflation with the role of a source of EDE, the potential necessitates another phase transition close to recombination. This secondary transition aims to mimic yet another lower cosmological constant, aligning with the present value of the Hubble rate and offering an alternative approach to mitigate the Hubble tension. In essence, our exploration of these alternative modifications within the quintessential inflation framework unfolds as an endeavor to enhance the concordance model and offer nuanced solutions to the intriguing cosmic puzzle presented by the Hubble tension.

This paper is organized as follows: In Section 2, we discuss various quintessential inflation models, starting with the original Peebles–Vilenkin model [53] and its companions. In Section 3, we discuss instant preheating, and in Section 4, we introduce gravitational reheating via particle production. Section 5 discusses the Hubble constant tension in the context of quintessential inflation. Finally, in Section 6, we close the present article, describing the key findings in short.

2. Quintessential Inflation: The Set-Up

Throughout this article, we use the spatially flat Friedmann–Lemaître–Robertson–Walker (FLRW) metric, with $a(t)$ representing the universe's scale factor. The core idea behind the theory of quintessential inflation is as follows: the inflation field is responsible for both the early and late-time acceleration of the universe. After inflation ends, there is a sudden phase transition leading to a period of kination (where the field's energy is purely kinetic, characterized by an EoS $w_{\rm eff} = 1$). This breaks the adiabatic evolution, enabling the creation of superheavy particles. The energy density of these particles (scaling as $\rho \sim a^{-3}$) eventually surpasses that of the inflation field (which scales as $\rho_\varphi \sim a^{-6}$) once they decay into lighter particles. This process transitions the universe into the radiation-dominated phase of the hot Big Bang. As the universe cools, particles become non-relativistic, leading to matter dominance. Eventually, in the present era, inflation's energy density rises again in the form of dark energy, known as quintessence, driving the current cosmic acceleration.

2.1. The Peebles–Vilenkin Quintessential Inflation

The first model of quintessential inflation, introduced by Peebles and Vilenkin in [53], contains the following potential:

$$V(\varphi) = \begin{cases} \lambda\left(\varphi^4 + M^4\right) & \text{for} \quad \varphi \leq 0 \\ \lambda \frac{M^8}{\varphi^4 + M^4} & \text{for} \quad \varphi \geq 0, \end{cases} \tag{1}$$

where λ is a dimensionless parameter and M is a very small mass compared with the reduced Planck's mass M_{pl} (i.e., $M \ll M_{pl}$). Note that the abrupt phase transition occurs at $\varphi = 0$, where the fourth derivative of V is discontinuous.

In this simplified model, the first part of the potential, the quartic term, drives inflation, while the inverse power law potential, forming the quintessence tail, is responsible for the current cosmic acceleration. As discussed in [53], the parameter $\lambda \cong 9 \times 10^{-11}$ is determined from the scalar perturbation power spectrum. The value of $M \sim 200$ TeV is derived from observational data, specifically from $\Omega_{\varphi,0} \equiv \frac{\rho_{\varphi,0}}{3H_0^2 M_{pl}^2} \cong 0.7$.

Considering that the inflationary component of the potential is quartic, a straightforward calculation reveals the relationship between the number of final e-folds (from horizon crossing to the end of inflation) and the spectral index:

$$N = \frac{6}{1 - n_s} - 2. \tag{2}$$

According to Planck 2018 data [39], the spectral index is measured to be $n_s = 0.9649 \pm 0.0042$. From (2) we can see that, at the 2σ confidence level, the number of e-folds is too high. It is bound by $136 \leq N \leq 223$, which shows that the Peebles–Vilenkin model is incompatible with the observational data, and thus it has to be ruled out.

Another way to disregard the model is considering the tensor/scalar ratio, which is given by $r = \frac{16}{3}(1 - n_s)$. Therefore, at a 2σ confidence level, the constraint is $0.1424 \leq r \leq 0.232$, which is inconsistent with the observational limit of $r \leq 0.1$ as reported by [39].

Improved Version: Starobinsky Inflation + Inverse Power Law

The problem in the Peebles–Vilenkin model is the quadratic potential responsible for inflation. Then, replacing it by a plateau-type potential, for example, the Starobinsky one (see, for instance, [113], one can obtain spectral values compatible with the observational data. Considering the potential

$$V(\varphi) = \begin{cases} \lambda M_{pl}^4 \left(1 - e^{\sqrt{\frac{2}{3}}\frac{\varphi}{M_{pl}}}\right)^2 + \lambda M^4 & \text{for} \quad \varphi \leq 0 \\ \lambda \frac{M^8}{\varphi^4 + M^4} & \text{for} \quad \varphi \geq 0, \end{cases} \tag{3}$$

one has the relation between the spectral index and the tensor/scalar ratio

$$r = 3(1 - n_s)^2 \Longrightarrow r < 5 \times 10^{-3},$$

which matches perfectly with Planck's data.

2.2. Lorentzian Quintessential Inflation

Based on the Lorentzian (Cauchy for Mathematicians) distribution, one considers the following *ansatz* [114]:

$$\epsilon(N) = \frac{\xi}{\pi} \frac{\Gamma/2}{N^2 + \Gamma^2/4}, \tag{4}$$

where ϵ denotes the main slow-roll parameter, N is once again the number of e-folds, ξ is the amplitude of the Cauchy distribution, and Γ is its width. We obtain the following potential [87]:

$$V(\varphi) = \lambda M_{pl}^4 \exp\left[-\frac{2\gamma}{\pi} \arctan\left(\sinh\left(\gamma\varphi/M_{pl}\right)\right)\right], \tag{5}$$

where λ is a dimensionless parameter, and the parameter γ is defined by $\gamma \equiv \sqrt{\frac{\pi}{\Gamma\xi}}$. In Figure 1, the evolution of this potential is depicted.

The model is governed by two parameters, and in order to align with current observational data, one must set $\lambda \sim 10^{-69}$ and $\gamma \cong 122$. This choice results in a successful inflationary phase and, at late times, leads to eternal cosmic acceleration with an effective EoS parameter equal to -1.

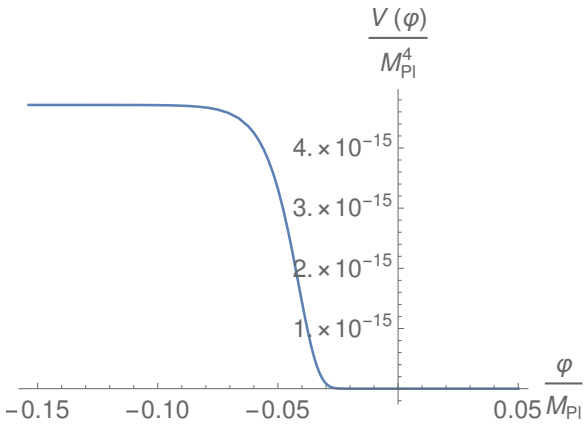

Figure 1. The shape of the potential in Lorentzian quintessential inflation. Inflation ends when $\varphi_{\rm END} \cong -0.078 M_{pl}$, and kination starts when $H \sim H_{\rm kin} \cong 4 \times 10^{-8} M_{\rm pl}$ with $\varphi_{\rm kin} \cong -0.03 M_{\rm pl}$. The figure has been taken from [89].

2.3. α-Attractors in Quintessential Inflation

The Lagrangian, depicting the evolution of a field under the action of an exponential potential, provided by super-symmetric gravity theories, is [115]

$$\mathcal{L} = \frac{1}{2} \frac{\dot{\phi}^2}{(1 - \frac{\phi^2}{6\alpha})^2} M_{pl}^2 - \lambda M_{pl}^4 e^{-\kappa \phi}, \tag{6}$$

where ϕ is a dimensionless scalar field, and κ and λ are positive dimensionless constants. In order that the kinetic term has the canonical form, i.e., $\frac{1}{2}\dot{\varphi}^2$, one can redefine the scalar field as follows:

$$\phi = \sqrt{6\alpha} \tanh\left(\frac{\varphi}{\sqrt{6\alpha} M_{pl}} \right) \tag{7}$$

obtaining the following potential [88,115]:

$$V(\varphi) = \lambda M_{pl}^4 e^{-n \tanh\left(\frac{\varphi}{\sqrt{6\alpha} M_{pl}} \right)}, \qquad n \equiv \kappa \sqrt{6\alpha}. \tag{8}$$

In Figure 2, we show the evolution of the effective EoS parameter $w_{\rm eff} = -1 - \frac{2\dot{H}}{3H^2}$ in terms of $N = \ln(a/a_0) = -\ln(1+z)$ (a_0 denotes the present value of the scale factor). The numerical integration begins at the start of kination, and it is observed at the present time, $w_{\rm eff} < -1/3$, indicating that the universe is accelerating. As time progresses, our universe transits to a de Sitter phase, where the equation of state parameter approaches to $w_{\rm eff} = -1$.

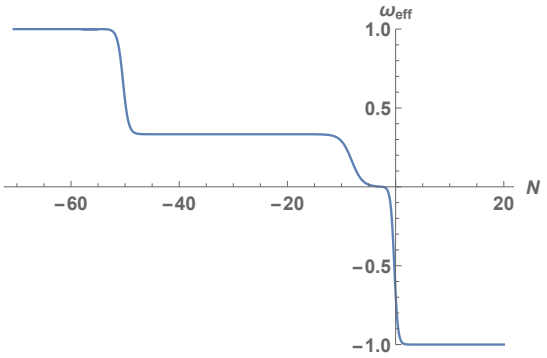

Figure 2. Evolution of the effective EoS parameter. The figure has been taken from [88].

3. Instant Preheating

The idea of instant preheating was presented in [101] as a mechanism to reheat the universe in standard inflation. Later, it has been proved that it is very useful in quintessential inflation [116]. Here, we will describe the basic ideas of this reheating mechanism:

First of all, we consider a quantum field, namely ϕ, responsible for particle production whose Lagrangian density is given by

$$\mathcal{L} = \frac{1}{2}\sqrt{|g|}(g^{\mu\nu}\partial_\mu\phi\partial_\nu\phi - \tilde{g}^2(\varphi - \varphi_{\rm kin})^2\phi^2 - \xi R\phi^2 + h\bar{\psi}\psi\phi), \tag{9}$$

where R denotes the scalar curvature, $\varphi_{\rm kin}$ is the value of the inflation at the onset of kination, $\tilde{g}$ is the dimensionless coupling constant between the inflation and the quantum field, and $h\bar{\psi}\psi\phi$ is the usual Yukawa interaction between the quantum field ϕ and fermions ψ [116]. Considering conformally coupled particles, i.e., when $\xi = 1/6$, the frequency of the k-modes is

$$\omega_k^2(\eta) = k^2 + m_{\rm eff}^2(\eta)a^2(\eta), \tag{10}$$

where $m_{\rm eff}(\eta) = \tilde{g}(\varphi(\eta) - \varphi_{\rm kin})$ is the effective mass of the produced particles, which grows during kination. In order to calculate analytically the Bogoliubov coefficients (the main ingredient to obtain the reheating temperature), we perform the linear approximation $\varphi(\eta) - \varphi_{\rm kin} \cong \varphi'_{\rm kin}(\eta - \eta_{\rm kin})$, and we assume that the universe is static with $a(\eta) = a_{\rm kin}$. Then, the frequency becomes

$$\omega_k^2(\eta) = k^2 + \tilde{g}^2 a_{\rm kin}^2(\varphi'_{\rm kin})^2(\eta - \eta_{\rm kin})^2. \tag{11}$$

Thus, using the complex WKB approximation, the analytic value of the β-Bogoliubov coefficients is given by [116]

$$|\beta_k|^2 \cong \exp\left(-\frac{\pi k^2}{\tilde{g}a_{\rm kin}\varphi'_{\rm kin}}\right) = \exp\left(-\frac{\pi k^2}{\sqrt{6}\tilde{g}a_{\rm kin}^2 H_{\rm kin}M_{pl}}\right). \tag{12}$$

Thus, the number density of produced particles at the onset of kination is

$$\langle\hat{N}_{\rm kin}\rangle = \frac{1}{2\pi^2 a_{\rm kin}^3}\int_0^\infty k^2|\beta_k|^2 dk = \frac{1}{8\pi^3}(\tilde{g}\sqrt{2\rho_{\rm B,kin}})^{3/2}, \tag{13}$$

where $\rho_{\rm B,kin} = 3H_{\rm kin}^2 M_{\rm pl}^2$ is the background energy density at the beginning of kination. Since the effective mass of the produced particles grows, they have to decay, with a decay rate $\Gamma \equiv \Gamma(\phi \to \psi\psi) \sim \frac{h^2\tilde{g}M_{\rm pl}}{8\pi}$ (see [116] for details) in lighter ones, which, after

thermalization, will reheat the universe. After some calculations, the reheating temperature is given by [117]

$$T_{\rm reh} \cong 3\times 10^{-3}\tilde{g}^{15/8}\left(\frac{M_{\rm pl}}{\bar{\Gamma}}\right)^{1/4}\ln^{3/4}\left(\frac{M_{\rm pl}}{\bar{\Gamma}}\right)M_{\rm pl}, \tag{14}$$

where we have introduced the notation $\bar{\Gamma}\equiv 10^7\Gamma$, Γ being the decay rate, and we have taken $H_{\rm kin}\sim 10^{-7}M_{\rm pl}$. To avoid problems such as the gravitino problem or the overproduction of gravitational waves, a successful reheating of the universe ($T_{\rm reh}\leq 10^9$ GeV) is achieved through the instant preheating mechanism when the value of the coupling constant satisfies $10^{-6}\leq\tilde{g}\leq 3\times 10^{-5}$ and the decay rate is $2\times 10^{33}\tilde{g}^{15/2}\leq\frac{\bar{\Gamma}}{M_{\rm pl}}<1/3$. For example, taking $\tilde{g}=6\times 10^{-6}$, we obtain

$$T_{\rm reh} \cong 5\times 10^{-13}\left(\frac{M_{\rm pl}}{\bar{\Gamma}}\right)^{1/4}\ln^{3/4}\left(\frac{M_{\rm pl}}{\bar{\Gamma}}\right)M_{\rm pl}, \tag{15}$$

with $10^{-6}\leq\frac{\bar{\Gamma}}{M_{\rm pl}}<1/3\Longrightarrow 10^{-13}\leq\frac{h^2\tilde{g}}{8\pi}<\frac{1}{3}\times 10^{-7}\Longrightarrow\frac{4\pi}{3}\times 10^{-7}\leq h^2<\frac{4\pi}{9}\times 10^{-1}$, which results in the following upper and lower bounds for the reheating temperatures:

$$T_{\rm reh}^{\rm max}\cong 10^9\ {\rm GeV}\qquad\text{and}\qquad T_{\rm reh}^{\rm min}\cong 10^6\ {\rm GeV}. \tag{16}$$

4. Gravitational Reheating

Gravitational reheating [102–105,118] is a compelling mechanism by which the interaction of a quantum field coupled with gravity generates heavy massive particles that decay into standard model (SM) particles and other forms of matter and radiation, thereby reheating the universe. Unlike conventional reheating scenarios that involve specific couplings between the inflation and other fields, gravitational reheating relies on the dynamics of the spacetime itself, making it a universal process that does not depend on the details of particle interactions.

In fact, at the Lagrangian level, the quantum field is coupled with the Ricci scalar, and since in quintessential inflation the adiabatic evolution is disrupted when the universe transitions from the inflationary epoch to the kination era, massive particles are produced during this phase transition.

The mode–frequency corresponding to heavy, massive particles conformally coupled with gravity is

$$\omega_k^2(\eta)=k^2+a^2(\eta)m_\chi^2, \tag{17}$$

where m_χ represents the mass of the produced particles. Defining "END" as the end of inflation, occurring when $\dot{H}=-H^2$ or equivalently when the principal slow-roll parameter ϵ equals one, if we expand the scale factor up to second order around this point using Taylor expansion, we obtain

$$a^2(\eta)\cong a_{\rm END}^2+2a_{\rm END}^3H_{\rm END}(\eta-\eta_{\rm END})+2a_{\rm END}^4H_{\rm END}^2(\eta-\eta_{\rm END})^2. \tag{18}$$

Then, inserting this last expression in (17), the frequency $\omega_k(\eta)$ can be approximated, up to order two around $\eta_{\rm END}$, by

$$\omega_k^2(\eta)\cong k^2+\frac{m_\chi^2a_{\rm END}^2}{2}+2a_{\rm END}^4H_{\rm END}^2m_\chi^2\left(\eta-\eta_{\rm END}+\frac{1}{2a_{\rm END}H_{\rm END}}\right)^2. \tag{19}$$

For this frequency, the β-Bogoliubov coefficient is

$$|\beta_k|^2 = \exp\Big(-\frac{\pi\left(k^2+\frac{a_{\rm END}^2 m_\chi^2}{2}\right)}{\sqrt{2}a_{\rm END}^2 m_\chi H_{\rm END}}\Big), \tag{20}$$

and the corresponding energy density at the onset of kination [118] is given by

$$\langle\rho_{kin}\rangle \cong \frac{1}{4\pi^3}e^{-\frac{\pi m_\chi}{2\sqrt{2}H_{\rm END}}}\sqrt{\frac{m_\chi}{\sqrt{2}H_{\rm END}}}H_{\rm END}^2 m_\chi^2, \tag{21}$$

demonstrating that the energy density of the produced particles decreases exponentially for masses greater than $H_{\rm END}$. To achieve a reheated universe, these particles have to decay in lighter ones. Then, using the Stefan–Boltzmann law $\rho_{\rm reh} = \frac{\pi^2 g_{\rm reh}}{30}T_{\rm reh}^4$, where $g_{\rm reh} \cong 107$ are the effective degrees of freedom for the standard model, the reheating temperature is given by (see [78,118] for details):

$$T_{\rm reh} = \left(\frac{10}{3\pi^2 g_{\rm reh}}\right)^{1/4}\left(\frac{\langle\rho_{kin}\rangle^3}{H_{\rm END}^3\Gamma M_{pl}^8}\right)^{1/4} M_{pl}, \tag{22}$$

where the decay rate, $\Gamma \sim \frac{h^2 m_\chi}{8\pi}$, has to satisfy

$$\frac{\langle\rho_{kin}\rangle}{3H_{\rm END}M_{pl}^2} \leq \Gamma \leq H_{\rm END}, \tag{23}$$

which results from the fact that $\Gamma \leq H_{\rm kin} \approx H_{\rm END}$ (indicating that decay occurs after the onset of kination) and $\langle\rho_{\rm dec}\rangle \leq 3\Gamma^2 M_{\rm pl}^2$ (indicating that decay occurs before the end of kination). The maximum reheating temperature, denoted as $T_{\rm reh}^{\rm max}$, is achieved when decay occurs at the end of kination. This is because, throughout the kination phase, the energy density of the produced particles scales as a^{-3} (and after decay, it scales as a^{-4}). Consequently, it quickly matches the energy density of the inflation. Therefore, by choosing $\Gamma = \frac{\langle\rho_{\rm kin}\rangle}{3H_{\rm END}M_{\rm pl}^2}$ and using the energy density of the produced particles (21), we can determine the maximum reheating temperature:

$$T_{\rm reh}^{\rm max}(m_\chi) \cong \frac{1}{5\pi^2}e^{-\frac{\pi m_\chi}{4\sqrt{2}H_{\rm END}}}\sqrt{\frac{H_{\rm END}}{M_{\rm pl}}}m_\chi. \tag{24}$$

The maximum reheating temperature depends on the mass of the particles, reaching its peak value when $m_\chi = \frac{4\sqrt{2}}{\pi}H_{\rm END}$. At this mass, the reheating temperature is approximately

$$T_{reh}^{max}\left(\frac{4\sqrt{2}}{\pi}H_{END}\right) \cong \frac{4\sqrt{2}}{5\pi^3 e}\sqrt{\frac{H_{END}}{M_{pl}}}H_{END}. \tag{25}$$

Then, for a typical Hubble rate at the end of inflation, approximately $H_{END} \sim 10^{-6}M_{pl}$, the maximum value is

$$T_{\rm reh}^{\rm max}\left(2\times 10^{-6}M_{\rm pl}\right) \cong 2\times 10^7\ \text{GeV}. \tag{26}$$

4.1. Application to α-Attractors

In the context of α-attractors (refer to the potential in (8)), we determine H_{END} analytically by computing the slow-roll parameter:

$$\epsilon = \frac{M_{pl}^2}{2}\left(\frac{V_\varphi}{V}\right)^2 = \frac{n^2}{12\alpha}\frac{1}{\cosh^4\left(\frac{\varphi}{\sqrt{6\alpha}M_{pl}}\right)}. \tag{27}$$

Since inflation ends when $\epsilon = 1$ and noting that $\text{arccosh}(x) = \ln(x - \sqrt{x^2-1})$, one has

$$\varphi_{END} = \sqrt{6\alpha}\ln\left(\frac{\sqrt{n}}{(12\alpha)^{1/4}} - \sqrt{\frac{n}{\sqrt{12\alpha}} - 1}\right)M_{pl}, \tag{28}$$

and thus,

$$V(\varphi_{END}) \cong \alpha 10^{-10} M_{pl}, \tag{29}$$

where, after using that $\rho_{END} = \frac{3V(\varphi_{END})}{2}$, one obtains

$$H_{END} \cong \sqrt{\frac{\alpha}{2}}10^{-5} M_{pl}. \tag{30}$$

Therefore, the maximum reheating temperature in the conformally coupled case is given by

$$T_{reh}^{max}(m_\chi) \cong 6\times 10^{-4}\left(\frac{\alpha}{2}\right)^{1/8}\exp\left(-\frac{\pi\times 10^5 m_\chi}{4\sqrt{\alpha}M_{pl}}\right)\left(\frac{m_\chi}{M_{pl}}\right)^{1/4} m_\chi, \tag{31}$$

which, for $\alpha = 10^{-2}$, becomes

$$T_{reh}^{max}(m_\chi) \cong 3\times 10^{-4}\exp\left(-\frac{\pi\times 10^6 m_\chi}{4M_{pl}}\right)\left(\frac{m_\chi}{M_{pl}}\right)^{1/4} m_\chi, \tag{32}$$

which, as we can see in Figure 3, matches very well with the numerical results.

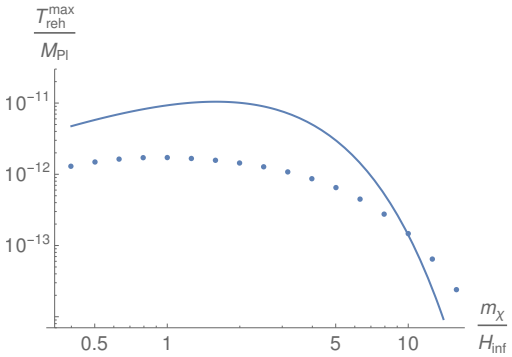

Figure 3. Numerical (in dots) and analytic values for the maximum reheating temperature. The values of the parameters are $H_{inf} = 10^{-6}M_{pl}$, $\alpha = 10^{-2}$, and $n = 124$. The figure has been taken from [118].

4.2. Relation Between the Number of Last e-Folds and the Reheating Temperature: α-Attractors

The well-known formula that relates the number of e-folds with the reheating temperature and the main slow-roll parameter is as follows (see [117] for details):

$$N(T_{\rm reh}, \epsilon_*) \cong 54.47 + \frac{1}{2}\ln\epsilon_* + \frac{1}{3}\ln\left(\frac{M_{\rm pl}^2}{T_{\rm reh}H_{\rm END}}\right), \tag{33}$$

where the $*$ means that the quantities are evaluated at the horizon crossing. Note that, to obtain this formula, we have disregarded the term $\ln\left(\frac{a_{\rm END}}{a_{\rm kin}}\right)$ since it is close to zero, and we have used that, in practice, the energy density does not change during the phase transition from the end of inflation to the onset of kination. On the other hand, for α-attractors, one has

$$N(n_s) \cong \frac{2}{1-n_s} \quad \text{and} \quad \epsilon_*(n_s) \cong \frac{3\alpha}{16}(1-n_s)^2. \tag{34}$$

Equaling (33) and (34), one finds the reheating temperature as a function of the spectral index as follows:

$$T_{reh} \cong \alpha(1-n_s)^2 \exp\left(169 + \frac{\sqrt{3\alpha}}{2} - \frac{6}{1-n_s}\right) M_{pl}. \tag{35}$$

Choosing, for example, $\alpha = 10^{-2}$, the reheating temperature will become

$$T_{\rm reh} \cong (1-n_s)^2 \exp\left(169 + \frac{\sqrt{3}}{20} - \frac{6}{1-n_s}\right) 10^{-2} M_{\rm pl}, \tag{36}$$

and the allowed values of n_s, which ensure a reheating temperature preserving with the BBN success ($T_{\rm reh} \geq 1$ MeV) and overpassing the gravitino problem ($T_{\rm reh} \leq 10^9$ GeV), belong in the range $(0.9665, 0.9709)$, which enters in the 95% confidence level of the observational data provided by Planck's team [108], because $n_s = 0.9649 \pm 0.0042$. In addition, the tensor/scalar ratio satisfies $r = 16\epsilon_* = 3\alpha(1-n_s)^2$, and thus, it is constrained by $0.000024 < r < 0.000034$. In particular, considering instant preheating, we have seen that the reheating temperature belongs to the domain 10^6 GeV $\leq T_{reh} \leq 10^9$ GeV, which constrains the spectral index residing in the narrow interval $(0.9667, 0.9677)$. However, the Atacama Cosmology Telescope (ACT) [41] provides $n_s = 0.9858^{+0.0051}_{-0.0030}$, which disfavors the α-attractors. We can see in Figure 4 that the same happens for the other inflationary potentials, such as Starobinsky and SUSY inflationary models (details can be found in [119]).

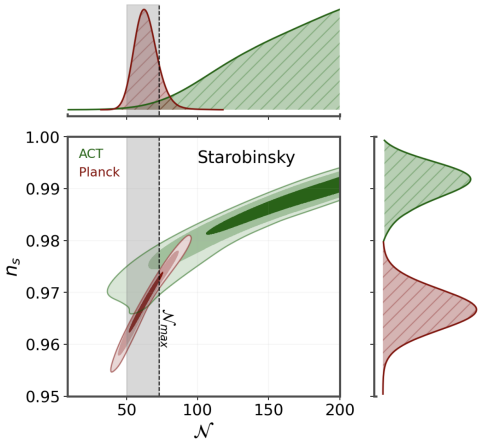

Figure 4. Two-dimensional contours at 68%, 95%, and 99% confidence levels in the (n_s, N) plane for the Starobinsky model. The gray vertical band indicates the typical range of e-folds expansion, $N \in [50, Nmax]$, expected during inflation. The upper bound, $Nmax \leq 73$, is shown by the black dashed line. This figure is adapted from [119].

Relation Between n_s and m_χ

Using the earlier result for the maximum reheating temperature (32) with $\alpha = 10^{-2}$, which solely depends on the mass of the produced particles, we derive the relationship between the spectral index and the mass of the particles produced:

$$\frac{2.6057}{1-n_s} - 1.75\log(1-n_s) = 79.301 + \frac{1.2398}{1-n_s}X - 1.25\log X, \tag{37}$$

where we have introduced the notation $X \equiv 10^4 \frac{m_\chi}{M_{pl}}$. For the minimum value of the spectral index, Equation (37) only has one solution, $X_{min} = \frac{1.25(1-n_s)}{1.2398}$, and by inserting it into (37), we obtain

$$\frac{2.6057}{1-n_s} - 0.5\log(1-n_s) = 80.5465. \tag{38}$$

The only solution to this equation is $\bar{n}_s \cong 0.9673$ because the function

$$\frac{2.6057}{1-n_s} - 0.5\log(1-n_s) \tag{39}$$

is increasing. And thus, for this minimum value of the spectral index, Equation (37) also has a unique solution: $m_\chi \cong 10^{-6} M_{pl}$, which leads to a maximum reheating temperature around 10^7 GeV. For values of n_s in the domain $(0.9673, 0.9709)$ where $n_s = 0.9709$ is the maximum allowed value (recall the Planck 2018 data $n_s = 0.9649 \pm 0.0042$ [39]), leading to a reheating temperature above 1 MeV, Equation (37) always has two solutions. For example, when $n_s = 0.9709$, we find $m_\chi \cong 3 \times 10^{-5} M_{\rm pl}$ and $m_\chi \cong 5 \times 10^{-15} M_{\rm pl}$, with a reheating temperature around 1 MeV. In other words, if the decay happens at the end of kination (resulting in the maximum reheating temperature), the spectral index must fall within the range $(0.9673, 0.9709)$, with two possible masses corresponding to each value. Alternatively, for masses within the range $5 \times 10^{-15} \leq m_\chi / M_{\rm pl} \leq 3 \times 10^{-5}$, there is a corresponding spectral index between 0.9673 and 0.9709, leading to a viable maximum reheating temperature.

5. H_0 Tension

The $\sim 5\sigma$ discrepancy between Planck (within ΛCDM) [108] and SH0ES [109] is a serious issue at the present moment, which suggests a possible revision of the ΛCDM cosmology. Various mechanisms are available to address the H_0 discrepancy (see [110–112]). Such modifications are either performed at the late time or during the early evolution of the universe; however, the actual truth is still unknown [110–112]. Adhering to the insights provided in [120] (refer to the beginning of Section II of [120]), it is elucidated that the parameter instrumental in constraining H_0 through observations of early universe physics is the angular scale of the sound horizon:

$$\theta_s(z_*) = \frac{r_s(z_*)}{D_A(z_*)}, \tag{40}$$

where z_* is the redshift at the baryon–photon decoupling and $D_A(z)$, the angular diameter distance, is defined by

$$D_A(z) = \int_0^z \frac{dz'}{H(z')}, \tag{41}$$

and the physical size of the sound horizon at the redshift z_* is

$$r_s(z_*) = \int_{z_*}^{\infty} \frac{c_s(z)}{H(z)} dz. \tag{42}$$

The speed of sound in the baryon–photon fluid is given by $c_s(z) \approx \left(3 + \frac{9\rho_b(z)}{4\rho_\gamma(z)}\right)^{-1/2}$, where $\rho_b(z)$ and $\rho_\gamma(z)$ represent the densities of baryons and photons at redshift z, respectively. Note that we can write

$$c_s(z) = \left(3\left(1 + \frac{3\Omega_{\mathrm{b},0}h^2}{4\Omega_{\mathrm{fl},0}h^2}\frac{1}{1+z}\right)\right)^{-1/2}, \tag{43}$$

and using the data $\Omega_{\mathrm{b},0}h^2 \cong 0.02237$ and $\frac{3}{4\Omega_{\mathrm{fl},0}h^2} \cong 31500$ [121], for $z \geq z_*$, one can safely make the approximation $c_s(z) \cong c_s(z_*) \cong 0.45$. In addition, for the ΛCDM model, denoting by H_Λ the Hubble rate for this model, one has

$$D_A^\Lambda(z_*) = \frac{\sqrt{3}}{M_{pl}}\int_0^{z_*} \frac{dz}{\sqrt{\rho_\Lambda + \rho_{\mathrm{m},0}(1+z)^3\left(1 + \frac{1+z}{1+z_{\mathrm{eq}}}\right)}} \tag{44}$$

which, at the time of baryon–photon decoupling, turns out to be $\cong 5.277 \times 10^{60} M_{\mathrm{pl}}^{-1}$ under the assumption of

$$\begin{aligned} \rho_{m,0} \cong 3.2877 \times 10^{-121} M_{pl}^4, \quad z_* = 1089.8, \quad z_{\mathrm{eq}} = 3387, \\ H_{\Lambda,0} = 67.66\ \mathrm{km/s/Mpc} \cong 5.9356 \times 10^{-61} M_{\mathrm{pl}}. \end{aligned} \tag{45}$$

Note that here, ρm, 0 denotes the present-day value of the matter density. Recall that, in the ΛCDM model, since the dark energy is denoted by $\rho_\Lambda = \Lambda M_{\mathrm{pl}}^2$, and since

$$3H_{\Lambda,0}^2 M_{\mathrm{pl}}^2 = \rho_\Lambda + \frac{2+z_{\mathrm{eq}}}{1+z_{\mathrm{eq}}}\rho_{\mathrm{m},0}, \tag{46}$$

we obtain $\rho_\Lambda \cong 7.3053 \times 10^{-121} M_{pl}^4$.

5.1. H_0 Tension in Quintessential Inflation: Inclusion of a Dynamical DE

Dealing with the exponential α-attractor

$$V(\varphi) = \lambda M_{\mathrm{pl}}^4 e^{-n\tanh\left(\frac{\varphi}{\sqrt{6\alpha}M_{\mathrm{pl}}}\right)}, \qquad n \equiv \kappa\sqrt{6\alpha}, \tag{47}$$

one approach to resolving the H_0 tension in quintessential inflation is to modify the expansion history for $z \lesssim 2$, adjusting the value of H_0 without altering the angular diameter distance at the time of last scattering. Since both quintessential inflation (for an exponential α-attractor) and ΛCDM predict the same value of $r_s(z_*)$ − as prior to the recombination epoch at z_*, the Hubble rate is mainly governed by matter and radiation energy densities—both models should yield the same angular diameter distance. However, since the energy density of the scalar field in quintessential inflation decreases, this match cannot be achieved. Therefore, to resolve the problem, one possible solution is to introduce a dynamical DE to modify the evolution of the universe at $z \lesssim 2$. The dynamical DE is not the only possibility to alleviate the H_0 tension; there are various ways to modify the expansion history of the universe [110]. However, at this moment, there is no perfect cosmological model that can solve the H_0 tension in agreement with other astronomical surveys. The dynamical DE is a very natural extension to the cosmological constant.

To follow this direction, we can consider a very well known dynamical DE EoS parameter [122,123]:

$$w_{\mathrm{de}}(z) = w_0 + \frac{z}{1+z}w_a. \tag{48}$$

where w_0 is the present value of $w_{\rm de}$, and w_a, a constant, characterizes the dynamical nature of $w_{\rm de}$. For example, $w_a = 0$ represents that $w_{\rm de}$ does not evolve with time. Then, using the conservation equation of the DE fluid

$$\frac{d\rho}{dz} = \frac{3}{1+z}\left(1 + w_0 + w_a - \frac{w_a}{1+z}\right)\rho, \tag{49}$$

one can find the evolution of the energy density as

$$\rho_{\rm de}(z) = \rho_{\rm de,0}(1+z)^{3(1+w_0+w_a)}e^{-3w_a\frac{z}{1+z}}. \tag{50}$$

Therefore, we obtain

$$D_A^{\varphi+\rm de}(z_*) = \frac{\sqrt{3}}{M_{\rm pl}}\int_0^{z_*} dz\left[\rho_{\varphi,0} + \rho_{\rm de}(z) + \rho_{\rm m,0}(1+z)^3\left(1 + \frac{1+z}{1+z_{\rm eq}}\right)\right]^{-\frac{1}{2}}, \tag{51}$$

where we now have three free parameters, namely $\rho_{\rm de,0}$, w_0, and w_a, with the constraint $\rho_{\varphi,0} + \rho_{\rm de,0} > \rho_\Lambda$ in order to increase the present value of the Hubble rate. Choosing $\rho_{\varphi,0} + \rho_{de,0} = 9.1 \times 10^{-121} M_{pl}^4$, where ρ_φ denotes the energy density of the φ-field, this leads to $H_{\varphi+de,0} = 6.4259 \times 10^{-61} M_{pl} \cong 73.25$km/s/Mpc.

Imposing $D_A^{\varphi+\rm de}(z_*) \cong D_A^{\Lambda}(z_*) \cong 5.277 \times 10^{60} M_{\rm pl}^{-1}$, we have obtained the following values:

1. Considering $\rho_{\varphi,0} = 7 \times 10^{-121} M_{\rm pl}^4$, one can approximate $w_0 \cong -4.6333$ and $w_a = -0.0333$. The approximate value of w_0 corresponds to a super phantom stage of the dark energy at the present epoch. However, we note that such a high negative value of w_0 arises because of the choice of $\rho_{\varphi,0}$. On the other hand, the present value of the effective EoS parameter $w_0^{\rm eff}$, which is encoded in the quintessential inflation field and the phantom field, is

$$w_0^{\rm eff} = \frac{-\rho_{\varphi,0} + w_0\rho_{\rm de,0}}{\rho_{\varphi,0} + \rho_{\rm de,0}} \cong -1.8384. \tag{52}$$

   In addition, $\rho_{\rm de}(z_*) \cong 10^{-154} M_{\rm pl}^4$, $\rho_{\rm de}(2) \cong 2 \times 10^{-127} M_{\rm pl}^4$, $\rho_{\rm de} \to 0$ as $z \to -1$.
2. When considering $\rho_{\varphi,0} = 6 \times 10^{-121} M_{\rm pl}^4$, one can approximate $w_0 \cong -1.9333$ and $w_a = -0.0333$. In that case, $w_0^{\rm eff} = -1.3179$, $\rho_{\rm de}(z_*) \cong 3 \times 10^{-130} M_{\rm pl}^4$, $\bar{\rho}_{\rm de}(2) \cong 10^{-122} M_{\rm pl}^4$, $\rho_{\rm de} \to 0$ as $z \to -1$.
3. On the other hand, if $\rho_{\varphi,0} = 5 \times 10^{-121} M_{\rm pl}^4$, $w_0 \cong -1.5333$ and $w_a = -0.0333$. In that case, $w_0^{\rm eff} = -1.2402$, $\rho_{\rm de}(z_*) \cong 3 \times 10^{-128} M_{\rm pl}^4$, $\rho_{\rm de}(2) \cong 10^{-122} M_{\rm pl}^4$, $\rho_{\rm de} \to 0$ as $z \to -1$.

Thus, it is clear to understand that depending on the strength of $\rho_{\varphi,0}$, the nature of w_0 and the effective EoS at the present epoch alter. This is a clear indication that depending on $\rho_{\varphi,0}$, one can expect a quintessential nature of w_0; however, the phantom behavior of DE can increase the expansion rate of the universe, and as a result of which, one can mitigate the H_0 tension [110]. Finally, since $w_a < 0$, for $z < 0$, hence, the effective EoS parameter of the total fluid, namely, $w^{\rm eff}(z)$, will eventually become positive, that is, the Big Rip singularity [124], a typical nature of phantom fluids, is forbidden because the fluid becomes non-phantom. To conclude this section, we would like to emphasize that addressing the H_0 tension may require going beyond general relativity. In particular, the inclusion of a dynamical DE in the context of $f(R)$ gravity [125] or the introduction of the matter creation process in modified gravity [126] can play an effective role in reconciling the H_0 tension.

5.2. Quintessential Inflation as a Source of EDE

Another popular alternative to reconcile the Hubble tension involves EDE [32,120,127–133]. The presence of EDE can reduce the size of the sound horizon at recombination by adding extra energy density before recombination. This increase in pre-recombination energy boosts the Hubble rate at the time of photon decoupling. As a result, to preserve consistency with the concordance model—where the angular scale stays unchanged—the present-day Hubble rate must be higher than in the ΛCDM model (However, at this point, the readers might be interested to know that all early-time modifications may not be sufficient to solve the Hubble tension [134,135]).

In quintessential inflation, to inject this extra energy density, we improve the exponential potential that appears in the Lagrangian (6) as follows:

$$V(\phi) = \bar{\lambda} e^{-\kappa\phi} e^{-\bar{\kappa}\frac{\phi-\phi_c}{6\alpha-\phi\phi_c}} M_{pl}^4, \tag{53}$$

which, in terms of the canonical field φ defined in (7), leads to the following (see Figure 5):

$$V(\varphi) = \bar{\lambda} e^{-n\tanh\left(\frac{\varphi}{\sqrt{6\alpha}M_{pl}}\right)} e^{-m\tanh\left(\frac{(\varphi-\varphi_c)}{\sqrt{6\alpha}M_{pl}}\right)} M_{pl}^4, \tag{54}$$

where $m = \frac{\bar{\kappa}}{\sqrt{6\alpha}}$ and $\phi_c = \sqrt{6\alpha}\tanh\left(\frac{\varphi_c}{\sqrt{6\alpha}M_{pl}}\right)$, with $\varphi_c \cong \left(-10 + 2\sqrt{\frac{2}{3}}\ln\left(\frac{M_{pl}}{T_{\rm reh}}\right)\right) M_{pl}$, is the value of the scalar field close to the matter–radiation equality, as has been shown in [90]. In fact, the phase transition at φ_c has to occur close to the recombination. Note that, at early times, the potential behaves like (47) with $\lambda = \bar{\lambda} e^m$. Well before the matter–radiation equality, the field freezes during the radiation phase, and the potential becomes $V(\varphi) = \bar{\lambda} e^{-(n-m)} M_{pl}^4$ with $w_\varphi \cong -1$, i.e., it acts as a cosmological constant; this becomes an injection of energy as in the EDE models, and soon after the field is greater than φ_c, it rolls down the potential, and the EoS parameter of the field goes to 1 because the field enters in a second kination phase, which disappears at the present time because the field freezes once again, recovering $w_\varphi = -1$, and the potential has the form $V(\varphi) = \bar{\lambda} e^{-(n+m)} M_{pl}^4$, becoming another smaller cosmological constant. More precisely, the model, after reheating, has to be understood as a dynamical cosmological constant, which changes its scale close to the recombination.

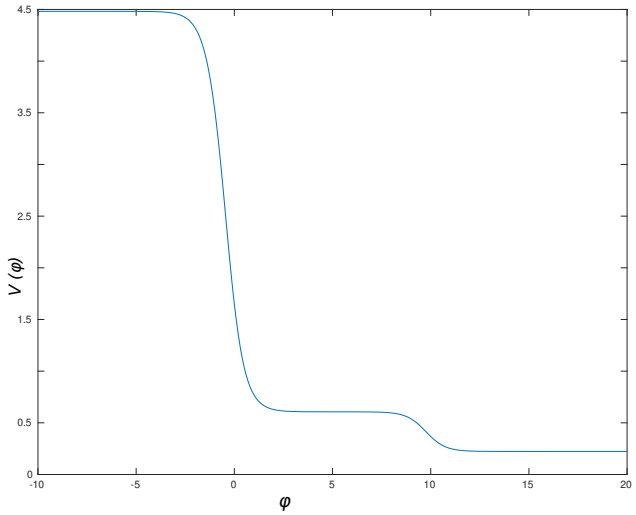

Figure 5. Plot of the potential (54) as a function of the field, taking some typical values of the parameters involved, namely, $\alpha = 1/6$, $\bar{\lambda} = 1$, $n = 1$, $m = 1/2$, and $\varphi_c = 10 M_{pl}$.

Qualitative Calculations

First of all, dealing with the concordance model, we write

$$H(z \leq z_*) \cong H_{\Lambda,0}\sqrt{\Omega_\Lambda + \Omega^\Lambda_{\mathrm{m},0}(1+z)^3}, \tag{55}$$

where we have introduced the notation $\Omega^\Lambda_{\mathrm{m},0} = \frac{\rho_{\mathrm{m},0}}{3H^2_{\Lambda,0}M^2_{\mathrm{pl}}}$, $\Omega_\Lambda = \frac{\rho_\Lambda}{3H^2_{\Lambda,0}M^2_{\mathrm{pl}}}$, and we have disregarded the radiation term, which is negligible for $z \leq z_*$. Thus,

$$D^\Lambda_A(z \leq z_*) \cong \frac{C}{H_{\Lambda,0}\Omega^{1/6}_\Lambda(\Omega^\Lambda_{m,0})^{1/3}}, \tag{56}$$

where

$$C = \int_{b_\Lambda}^{b_\Lambda(1+z_*)} \frac{dx}{\sqrt{1+x^3}} \quad \text{with} \quad b_\Lambda \equiv \left(\frac{\Omega^\Lambda_{\mathrm{m},0}}{\Omega_\Lambda}\right)^{1/3} \cong 0.75. \tag{57}$$

On the other hand, for $z_{\mathrm{eq}} \gg z \geq z_*$, one has $\Omega^\Lambda_{\mathrm{m},0}(1+z)^3 \gg \Omega_\Lambda$, and thus

$$H(z) \cong H_{\Lambda,*}\sqrt{\Omega^\Lambda_{m,*}}\left(\frac{z}{z_*}\right)^{3/2}, \tag{58}$$

where $H_{\Lambda,*} = H_\Lambda(z_*)$ and $\Omega^\Lambda_{\mathrm{m},*} = \frac{\rho_{\mathrm{m},0}(1+z_*)^3}{3H^2_{\Lambda,*}M^2_{pl}}$. Therefore, since, for $z \geq z_*$, one has $c_s(z) \cong c_s(z_*)$, one can make the approximation

$$r_s(z_*) \cong \frac{2c_s(z_*)z_*}{H_{\Lambda,*}\sqrt{\Omega^\Lambda_{m,*}}}, \tag{59}$$

and using the relationship $\Omega^\Lambda_{m,*} \cong \Omega^\Lambda_{m,0}\left(\frac{H_{\Lambda,0}}{H_{\Lambda,*}}\right)^2 z^3_*$, we obtain the following expression of the angular scale of the sound horizon:

$$\theta(z_*) \cong \frac{2c_s(z_*)}{C\sqrt{z_*}}\left(\frac{\Omega_\Lambda}{\Omega^\Lambda_{m,0}}\right)^{1/6}. \tag{60}$$

Dealing with quintessential inflation, in the same way as for the concordance model, we have

$$D^\varphi_A(z \leq z_*) \cong \frac{\bar{C}}{H_{\varphi,0}\Omega^{1/6}_{\varphi,0}(\Omega^\varphi_{m,0})^{1/3}}, \tag{61}$$

where

$$\bar{C} = \int_{b_\varphi}^{b_\varphi(1+z_*)} \frac{dx}{\sqrt{1+x^3}} \quad \text{with} \quad b_\varphi = \left(\frac{\Omega^\varphi_{m,0}}{\Omega_{\varphi,0}}\right)^{1/3}, \tag{62}$$

and we have introduced the notation $\Omega^\varphi_{\mathrm{m},0} = \frac{\rho_{\mathrm{m},0}}{3H^2_{\varphi,0}M^2_{\mathrm{pl}}}$, $\Omega_{\varphi,0} = \frac{\rho_{\varphi,0}}{3H^2_{\varphi,0}M^2_{\mathrm{pl}}}$. On the other hand, for $z_* \leq z \ll z_{\mathrm{eq}}$, we have

$$H(z) \cong H_{\varphi,*}\sqrt{\Omega_{\varphi,*} + \Omega^\varphi_{\mathrm{m},*}\left(\frac{1+z}{1+z_*}\right)^3}, \tag{63}$$

and thus,

$$r_s(z_*) \cong \frac{c_s(z_*) z_* D}{H_{\varphi,*} \Omega_{\varphi,*}^{1/6} (\Omega_{\mathrm{m},*}^{\varphi})^{1/3}}, \tag{64}$$

where

$$D = \int_{b_\varphi}^{\infty} \frac{dx}{\sqrt{1+x^3}} \qquad \text{with} \qquad b_\varphi = \left(\frac{\Omega_{\mathrm{m},*}^{\varphi}}{\Omega_{\varphi,*}} \right)^{1/3}. \tag{65}$$

Now, using $\Omega_{\mathrm{m},*}^{\varphi} \cong \Omega_{\mathrm{m},0}^{\varphi} \left(\frac{H_{\varphi,0}}{H_{\varphi,*}} \right)^2 z_*^3$, we obtain

$$\theta(z_*) \cong \frac{D c_s(z_*)}{\bar{C}} \left(\frac{\rho_{\varphi,0}}{\rho_{\varphi,*}} \right)^{1/6}. \tag{66}$$

Next, equaling the corresponding angular scales, i.e., Equation (60) with Equation (66), we obtain

$$\rho_{\varphi,*} \cong \frac{z_*^3}{64} \left(\frac{DC}{\bar{C}} \right)^6 \frac{\Omega_{\mathrm{m},0}^{\Lambda}}{1 - \Omega_{m,0}^{\Lambda}} \rho_{\varphi,0}, \tag{67}$$

where, taking into account that $C \cong \bar{C}$, $\Omega_{\mathrm{m},0}^{\Lambda} \cong 0.3$, $z_* \cong 1089$ and making the approximation $D \sim \int_1^{\infty} x^{-3/2} = 2$, we have

$$\rho_{\varphi,*} \sim 5 \times 10^8 \rho_{\varphi,0} \Longleftrightarrow V_* \sim 5 \times 10^8 V_0. \tag{68}$$

Choosing $V_0 \cong 9.1 \times 10^{-121} M_{\mathrm{pl}}^4$ to obtain $H_{\varphi,0} \cong 73$ km/s/Mpc, we have $V_* \sim 5 \times 10^{-112} M_{\mathrm{pl}}^4$. That is,

$$\bar{\lambda} e^{-(n+m)} \sim 9 \times 10^{-121}, \qquad \bar{\lambda} e^{-(n-m)} \sim 5 \times 10^{-112}, \tag{69}$$

which implies $m \sim 10$. On the other hand, using the formula of the power spectrum of scalar perturbations [136], we have

$$\bar{\lambda} \sim 9\alpha (1 - n_s)^2 \times 10^{-9} e^{-(n+m)}, \tag{70}$$

and choosing $\alpha \sim 10^{-2}$ and $1 - n_s \sim 10^{-2}$, we obtain $n \sim 112$.

6. Conclusions

A unified prescription connecting the early inflationary phase and late quintessential era, in terms of quintessential inflation, is the main theme of the present article, where we have focused on two important aspects of modern cosmology, namely, the reheating and the Hubble constant tension. One of the novelties of the present work is to discuss whether the Hubble constant tension can be alleviated within the framework of quintessential inflation, which has received considerable attention in the last couple of years.

We started with the review of the most important reheating mechanisms in quintessential inflation, namely instant preheating and gravitational reheating via the production of heavy particles, obtaining the reheating temperature in terms of the decay rate of these massive particles. After obtaining the reheating temperature, we have related it to the number of e-folds, which constrains the spectral index of scalar perturbations. Additionally, in the case of gravitational reheating and dealing with α-attractors coming from supersymmetric gravity theories, we have related the masses of the produced particles with the spectral index, obtaining the viable values of these masses, which are compatible, at the

2σ confidence level, with the observational values of the spectral index provided by the Planck team [39].

Next, we have analyzed some possible solutions to the H_0 tension in the context of quintessential inflation. Dealing with an exponential α-attractor representing a quintessential inflation model, since at late times it acts as a cosmological constant, we find that the quintessential inflation model alone is not able to increase the H_0 value, but a possibility to alleviate the H_0 tension is to introduce a dynamical DE that only acts at low redshift $z \leq 2$ with phantom nature at present time. In addition, for redshifts close to -1, the effective nature of the phantom fluid becomes non-phantom, which prevents the Big Rip singularity that arises in the presence of a phantom fluid [124]. Another possibility is to consider an exponential type of potential (54) where it acts as a source of EDE. In fact, after reheating, the potential acts as a cosmological constant, which, after a phase transition close to the recombination epoch, decays in another one.

In summary, this article emphasizes several key characteristics of models within the framework of quintessential inflation. Notably, addressing the Hubble constant tension is a novel topic in this context. Based on our review, this is the first instance where the question is posed as to whether the quintessential inflation models might provide a potential solution to the Hubble tension. We believe it is crucial to further investigate this issue within this framework using the observational data from various astronomical surveys.

Author Contributions: Methodology, J.d.H. and S.P.; Writing–review and editing, J.d.H. and S.P. All authors have read and agreed to the published version of the manuscript.

Funding: The research of JdH has been funded by the Spanish grants PID2021-123903NB-I00 and RED2022-134784-T given by MCIN/AEI/10.13039/501100011033 and ERDF "A way of making Europe". The research of SP has been funded by the Department of Science and Technology (DST), Govt. of India, under the scheme "Fund for Improvement of S&T Infrastructure (FIST)" (File No. SR/FST/MS-I/2019/41).

Data Availability Statement: The datasets which have been referred to this article are publicly available.

Acknowledgments: We thank the referees for their useful comments.

Conflicts of Interest: The authors declare no conflicts of interest.

References

1. Guth, A.H. The Inflationary Universe: A Possible Solution to the Horizon and Flatness Problems. *Phys. Rev. D* **1981**, *23*, 347–356. [CrossRef]
2. Linde, A.D. A New Inflationary Universe Scenario: A Possible Solution of the Horizon, Flatness, Homogeneity, Isotropy and Primordial Monopole Problems. *Phys. Lett. B* **1982**, *108*, 389–393. [CrossRef]
3. Barrow, J.D.; Turner, M.S. Inflation in the Universe. *Nature* **1981**, *292*, 35–38. [CrossRef]
4. Lucchin, F.; Matarrese, S. Power Law Inflation. *Phys. Rev. D* **1985**, *32*, 1316. [CrossRef]
5. Burd, A.B.; Barrow, J.D. Inflationary Models with Exponential Potentials. *Nucl. Phys. B* **1988**, *308*, 929–945; Erratum in *Nucl. Phys. B* **1989**, *324*, 276–276. [CrossRef]
6. Barrow, J.D.; Maeda, K.I. Extended inflationary universes. *Nucl. Phys. B* **1990**, *341*, 294–308. [CrossRef]
7. Freese, K.; Frieman, J.A.; Olinto, A.V. Natural inflation with pseudo—Nambu-Goldstone bosons. *Phys. Rev. Lett.* **1990**, *65*, 3233–3236. [CrossRef]
8. Barrow, J.D. New types of inflationary universe. *Phys. Rev. D* **1993**, *48*, 1585–1590. [CrossRef]
9. Barrow, J.D. Exact inflationary universes with potential minima. *Phys. Rev. D* **1994**, *49*, 3055–3058. [CrossRef]
10. Parsons, P.; Barrow, J.D. Generalized scalar field potentials and inflation. *Phys. Rev. D* **1995**, *51*, 6757–6763. [CrossRef]
11. Barrow, J.D.; Parsons, P. Inflationary models with logarithmic potentials. *Phys. Rev. D* **1995**, *52*, 5576–5587. [CrossRef] [PubMed]
12. Boubekeur, L.; Lyth, D.H. Hilltop inflation. *JCAP* **2005**, *7*, 010. [CrossRef]
13. Martin, J.; Ringeval, C. Inflation after WMAP3: Confronting the Slow-Roll and Exact Power Spectra to CMB Data. *JCAP* **2006**, *8*, 9. [CrossRef]
14. Barrow, J.D.; Liddle, A.R.; Pahud, C. Intermediate inflation in light of the three-year WMAP observations. *Phys. Rev. D* **2006**, *74*, 127305. [CrossRef]
15. Barrow, J.D.; Nunes, N.J. Dynamics of Logamediate Inflation. *Phys. Rev. D* **2007**, *76*, 043501. [CrossRef]

16. Sebastiani, L.; Cognola, G.; Myrzakulov, R.; Odintsov, S.D.; Zerbini, S. Nearly Starobinsky inflation from modified gravity. *Phys. Rev. D* **2014**, *89*, 023518. [CrossRef]
17. Kehagias, A.; Moradinezhad Dizgah, A.; Riotto, A. Remarks on the Starobinsky model of inflation and its descendants. *Phys. Rev. D* **2014**, *89*, 043527. [CrossRef]
18. Freese, K.; Kinney, W.H. Natural Inflation: Consistency with Cosmic Microwave Background Observations of Planck and BICEP2. *JCAP* **2015**, *3*, 044. [CrossRef]
19. Barrow, J.D.; Paliathanasis, A. Observational Constraints on New Exact Inflationary Scalar-field Solutions. *Phys. Rev. D* **2016**, *94*, 083518. [CrossRef]
20. Ooba, J.; Ratra, B.; Sugiyama, N. Planck 2015 Constraints on the Non-flat ΛCDM Inflation Model. *Astrophys. J.* **2018**, *864*, 80. [CrossRef]
21. Giarè, W.; Di Valentino, E.; Melchiorri, A. Testing the inflationary slow-roll condition with tensor modes. *Phys. Rev. D* **2019**, *99*, 123522. [CrossRef]
22. Anber, M. M.; Baker, S. Natural inflation, strong dynamics, and the role of generalized anomalies. *Phys. Rev. D* **2020**, *102*, 103515. [CrossRef]
23. Aoki, S.; Lee, H-M.; Menkara, A G. Inflation and supersymmetry breaking in Higgs-R^2 supergravity. *JHEP* **2021**, *10*, 178. [CrossRef]
24. Forconi, M.; Giarè, W.; Di Valentino, E.; Melchiorri, A. Cosmological constraints on slow roll inflation: An update. *Phys. Rev. D* **2021**, *104*, 103528. [CrossRef]
25. Schimmrigk, R. Large and small field inflation from hyperbolic sigma models. *Phys. Rev. D* **2022**, *105*, 063541. [CrossRef]
26. Bahr-Kalus, B.; Parkinson, D.; Easther, R. Constraining cosmic inflation with observations: Prospects for 2030. *Mon. Not. Roy. Astron. Soc.* **2023**, *520*, 2405–2416. [CrossRef]
27. He, M.; Hong, M.; Mukaida, K. Starobinsky inflation and beyond in Einstein-Cartan gravity. *JCAP* **2024**, *5*, 107. [CrossRef]
28. Lorenzoni, D.L.; Kaiser, D.I.; McDonough, E. Natural inflation with exponentially small tensor-to-scalar ratio. *Phys. Rev. D* **2024**, *110*, L061302. [CrossRef]
29. Martin, J.; Ringeval, C.; Vennin, V. Encyclopædia Inflationaris. *Phys. Dark Univ.* **2014**, *5–6*, 75–235. [CrossRef]
30. Odintsov, S.D.; Oikonomou, V.K.; Giannakoudi, I.; Fronimos, F.P.; Lymperiadou, E.C. Recent Advances in Inflation. *Symmetry* **2023**, *15*, 1701. [CrossRef]
31. Ellis, J.; Wands, D. Inflation (2023). *arXiv* **2023**, arXiv:2312.13238v1. https://arxiv.org/abs/2312.13238.
32. Giarè, W. Inflation, the Hubble tension, and early dark energy: An alternative overview. *Phys. Rev. D* **2024**, *109*, 123545, [CrossRef]
33. Fixsen, D.J.; Cheng, E.S.; Cottingham, D.A.; Eplee, R.E., Jr.; Isaacman, R.B. Cosmic microwave background dipole spectrum measured by the COBE FIRAS. *Astrophys. J.* **1994**, *420*, 445. [CrossRef]
34. Bennett, C.L.; Banday, A.; Gorski, K.M.; Hinshaw, G.; Jackson, P.; Keegstra, P.; Kogut, A.; Smoot, G.F.; Wilkinson, D.T.; Wright, E.L. Four year COBE DMR cosmic microwave background observations: Maps and basic results. *Astrophys. J. Lett.* **1996**, *464*, L1–L4. [CrossRef]
35. Peiris1, H.V.; Komatsu1, E.; Verde1, L.; Spergel1, D.N.; Bennett, C.L.; Halpern, M.; Hinshaw, G.; Jarosik, N.; Kogut, A.; Limon, M.; et al. First year Wilkinson Microwave Anisotropy Probe (WMAP) observations: Implications for inflation. *Astrophys. J. Suppl.* **2003**, *148*, 213–231. [CrossRef]
36. Bennett1, C.L.; Larson1, D.; Weiland1, J.L.; Jarosik, N.; Hinshaw, G.; Odegard, N.; Smith, K.M.; Hill, R.S.; Gold, B.; Halpern, M.; et al. Nine-Year Wilkinson Microwave Anisotropy Probe (WMAP) Observations: Final Maps and Results. *Astrophys. J. Suppl.* **2013**, *208*, 20. [CrossRef]
37. Ade, P.A.R.; Aghanim, N.; Armitage-Caplan, C.; Arnaud, M.; Ashdown, M.; Atrio-Barandela, F.; Aumont, J.; Baccigalupi, C.; Banday, A.J.; Barreiro, R.B.; et al. Planck 2013 results. XXII. Constraints on inflation. *Astron. Astrophys.* **2014**, *571*, A22. [CrossRef]
38. Ade, P.A.R.; Aghanim, N.; Armitage-Caplan, C.; Arnaud, M.; Ashdown, M.; Atrio-Barandela, F.; Aumont, J.; Baccigalupi, C.; Banday, A.J.; Barreiro, R.B.; et al. Planck 2015 results. XX. Constraints on inflation. *Astron. Astrophys.* **2016**, *594*, A20. [CrossRef]
39. Akrami, Y.; Arroja, F.; Ashdown, M.; Aumont, J.; Baccigalupi, C.; Ballardini, M.; Banday, A.J.; Barreiro, R.B.; Bartolo, N.; Basak, S.; et al. Planck 2018 results. X. Constraints on inflation. *Astron. Astrophys.* **2020**, *641*, A10. [CrossRef]
40. Aghanim, N.; Akrami, Y.; Ashdown, M.; Aumont, J.; Baccigalupi, C.; Ballardini, M.; Banday, A.J.; Barreiro, R.B.; Bartolo, N.; Basak, S.; et al. Planck 2018 results. V. CMB power spectra and likelihoods. *Astron. Astrophys.* **2020**, *641*, A5. [CrossRef]
41. Choi, S.K.; Hasselfield, M.; Ho, S.P.; Koopman, B.; Lungu, M.; Abitbol, M.H.; Addison, G.E.; Ade, P.A.R.; Aiola, S.; Alonso, D. The Atacama Cosmology Telescope: A measurement of the Cosmic Microwave Background power spectra at 98 and 150 GHz. *JCAP* **2020**, *12*, 45. [CrossRef]
42. Benson, B.A.; Ade, P.A.R.; Ahmed, Z.; Allen, S.W.; Arnold, K.; Austermann, J.E.; Bender, A.N.; Bleem, L.E.; Carlstrom, J.E.; Chang, C.L.; et al. SPT-3G: A Next-Generation Cosmic Microwave Background Polarization Experiment on the South Pole Telescope. *Proc. SPIE Int. Soc. Opt. Eng.* **2014**, *9153*, 91531P. [CrossRef]
43. Dutcher, D.; Balkenhol, L.; Ade, P.A.R.; Ahmed, Z.; Anderes, E.; Anderson, A.J.; Archipley, M.; Avva, J.S.; Aylor, K.; Barry, P.S. Measurements of the E-mode polarization and temperature-E-mode correlation of the CMB from SPT-3G 2018 data. *Phys. Rev. D* **2021**, *104*, 022003. [CrossRef]

44. Balkenhol, L.; Dutcher, D.; Spurio Mancini, A.; Doussot, A.; Benabed, K.; Galli, S.; Ade, A.D.E.; Anderson, A.J.; Ansarinejad, B.; Archipley, M.; et al. Measurement of the CMB temperature power spectrum and constraints on cosmology from the SPT-3G 2018 TT, TE, and EE dataset. *Phys. Rev. D* **2023**, *108*, 023510. [CrossRef]
45. Riess, A.G.; Filippenko, A.V.; Challis, P.; Clocchiatti, A.; Diercks, A.; Garnavich, P.M.; Gilliland, R.L.; Hogan, C.J.; Jha, S.; Kirshner, R.P.; et al. Observational evidence from supernovae for an accelerating universe and a cosmological constant. *Astron. J.* **1998**, *116*, 1009–1038. [CrossRef]
46. Perlmutter, S.; Aldering1, G.; Goldhaber, G.; Knop1, R.A.; Nugent, P.; Castro, P.G.; Deustua1, S.; Fabbro1, S.; Goobar, A.; Groom, D.E.; et al. Measurements of Ω and Λ from 42 high redshift supernovae. *Astrophys. J.* **1999**, *517*, 565–586. [CrossRef]
47. Caldwell, R.R.; Dave, R.; Steinhardt, P.J. Cosmological imprint of an energy component with general equation of state. *Phys. Rev. Lett.* **1998**, *80*, 1582–1585. [CrossRef]
48. Carroll, S.M. Quintessence and the rest of the world. *Phys. Rev. Lett.* **1998**, *81*, 3067–3070. [CrossRef]
49. Tsujikawa, S. Quintessence: A Review. *Class. Quant. Grav.* **2013**, *30*, 214003. [CrossRef]
50. Chimento, L.; Forte, M. Unified model of baryonic matter and dark components. *Phys. Lett. B* **2008**, *666*, 205–211. [CrossRef]
51. Gao, C.; Kunz, M.; Liddle, A.R.; Parkinson, D. Unified dark energy and dark matter from a scalar field different from quintessence. *Phys. Rev. D* **2010**, *81*, 043520. [CrossRef]
52. Luongo, O.; Mengoni, T. Quasi-quintessence inflation with non-minimal coupling to curvature in the Jordan and Einstein frames. *arxiv* **2023**, arXiv:2309.03065
53. Peebles, P.J.E.; Vilenkin, A. Quintessential inflation. *Phys. Rev. D* **1999**, *59*, 063505. [CrossRef]
54. Peloso, M.; Rosati, F. On the construction of quintessential inflation models. *JHEP* **1999**, *12*, 026. [CrossRef]
55. Giovannini, M. Spikes in the relic graviton background from quintessential inflation. *Class. Quant. Grav.* **1999**, *16*, 2905–2913. [CrossRef]
56. Kaganovich, A.B. Field theory model giving rise to 'quintessential inflation' without the cosmological constant and other fine tuning problems. *Phys. Rev. D* **2001**, *63*, 025022. [CrossRef]
57. Dimopoulos, K. Towards a model of quintessential inflation. *Nucl. Phys. B Proc. Suppl.* **2001**, *95*, 70–73. [CrossRef]
58. Yahiro, M.; Mathews, G.J.; Ichiki, K.; Kajino, T.; Orito, M. Constraints on cosmic quintessence and quintessential inflation. *Phys. Rev. D* **2002**, *65*, 063502. [CrossRef]
59. Dimopoulos, K.; Valle, J.W.F. Modeling quintessential inflation. *Astropart. Phys.* **2002**, *18*, 287–306. [CrossRef]
60. Campos, A.H.; Reis, H.C.; Rosenfeld, R. Preheating in quintessential inflation. *Phys. Lett. B* **2003**, *575*, 151–156. [CrossRef]
61. Nunes, N.J.; Copeland, E.J. Tracking quintessential inflation from brane worlds. *Phys. Rev. D* **2002**, *66*, 043524. [CrossRef]
62. Giovannini, M. Low scale quintessential inflation. *Phys. Rev. D* **2003**, *67*, 123512. [CrossRef]
63. Tashiro, H.; Chiba, T.; Sasaki, M. Reheating after quintessential inflation and gravitational waves. *Class. Quant. Grav.* **2004**, *21*, 1761–1772. [CrossRef]
64. Sami, M.; Sahni, V. Quintessential inflation on the brane and the relic gravity wave background. *Phys. Rev. D* **2004**, *70*, 083513. [CrossRef]
65. Rosenfeld, R.; Frieman, J.A. A Simple model for quintessential inflation. *JCAP* **2005**, *09*, 003. [CrossRef]
66. Zhai, X.h.; Zhao, Y.b. Dynamics of quintessential inflation. *Chin. Phys.* **2006**, *15*, 2465. [CrossRef]
67. Cardenas, V.H. Tachyonic quintessential inflation. *Phys. Rev. D* **2006**, *73*, 103512. [CrossRef]
68. Membiela, A.; Bellini, M. Quintessential inflation from a variable cosmological constant in a 5D vacuum. *Phys. Lett. B* **2006**, *641*, 125–129. [CrossRef]
69. Neupane, I.P. Reconstructing a model of quintessential inflation. *Class. Quant. Grav.* **2008**, *25*, 125013. [CrossRef]
70. Bento, M.C.; Gonzalez Felipe, R.; Santos, N.M.C. A simple quintessential inflation model. *Int. J. Mod. Phys. A* **2009**, *24*, 1639–1642. [CrossRef]
71. Hossain, M.W.; Myrzakulov, R.; Sami, M.; Saridakis, E.N. Class of quintessential inflation models with parameter space consistent with BICEP2. *Phys. Rev. D* **2014**, *89*, 123513. [CrossRef]
72. Geng, C.Q.; Hossain, M.W.; Myrzakulov, R.; Sami, M.; Saridakis, E.N. Quintessential inflation with canonical and noncanonical scalar fields and Planck 2015 results. *Phys. Rev. D* **2015**, *92*, 023522. [CrossRef]
73. de Haro, J.; Amorós, J.; Pan, S. Simple inflationary quintessential model. *Phys. Rev. D* **2016**, *93*, 084018. [CrossRef]
74. Guendelman, E.; Nissimov, E.; Pacheva, S. Quintessential Inflation, Unified Dark Energy and Dark Matter, and Higgs Mechanism. *Bulg. J. Phys.* **2017**, *44*, 015–030.
75. de Haro, J.; Elizalde, E. Inflation and late-time acceleration from a double-well potential with cosmological constant. *Gen. Rel. Grav.* **2016**, *48*, 77. [CrossRef]
76. de Haro, J. On the viability of quintessential inflation models from observational data. *Gen. Rel. Grav.* **2017**, *49*, 6. [CrossRef]
77. Geng, C.Q.; Lee, C.C.; Sami, M.; Saridakis, E.N.; Starobinsky, A.A. Observational constraints on successful model of quintessential Inflation. *JCAP* **2017**, *6*, 11. [CrossRef]
78. Aresté Saló, L.; de Haro, J. Quintessential inflation at low reheating temperatures. *Eur. Phys. J. C* **2017**, *77*, 798. [CrossRef]
79. Haro, J.; Pan, S. Bulk viscous quintessential inflation. *Int. J. Mod. Phys. D* **2018**, *27*, 1850052. [CrossRef]
80. Agarwal, A.; Myrzakulov, R.; Sami, M.; Singh, N.K. Quintessential inflation in a thawing realization. *Phys. Lett. B* **2017**, *770*, 200–208. [CrossRef]

81. Bettoni, D.; Domènech, G.; Rubio, J. Gravitational waves from global cosmic strings in quintessential inflation. *JCAP* **2019**, *2*, 34. [CrossRef]
82. Dimopoulos, K.; Karčiauskas, M.; Owen, C. Quintessential inflation with a trap and axionic dark matter. *Phys. Rev. D* **2019**, *100*, 083530. [CrossRef]
83. Haro, J.; Amorós, J.; Pan, S. Scaling solutions in quintessential inflation. *Eur. Phys. J. C* **2020**, *80*, 404. [CrossRef]
84. Verner, S. Quintessential Inflation in Palatini Gravity. *JCAP* **2021**, *4*, 001. [CrossRef]
85. Benisty, D.; Guendelman, E.I. Lorentzian Quintessential Inflation. *Int. J. Mod. Phys. D* **2020**, *29*, 2042002. [CrossRef]
86. Dimopoulos, K.; Sánchez López, S. Quintessential inflation in Palatini $f(R)$ gravity. *Phys. Rev. D* **2021**, *103*, 043533. [CrossRef]
87. Aresté Saló, L.; Benisty, D.; Guendelman, E.I.; Haro, J.d. Quintessential inflation and cosmological seesaw mechanism: Reheating and observational constraints. *JCAP* **2021**, *7*, 007. [CrossRef]
88. Aresté Saló, L.; Benisty, D.; Guendelman, E.I.; de Haro, J. α-attractors in quintessential inflation motivated by supergravity. *Phys. Rev. D* **2021**, *103*, 123535. [CrossRef]
89. Saló, L.A.; de Haro, J. Gravitational particle production of superheavy massive particles in quintessential inflation: A numerical analysis. *Phys. Rev. D* **2021**, *104*, 083544. [CrossRef]
90. de Haro, J.; Saló, L.A. A Review of Quintessential Inflation. *Galaxies* **2021**, *9*, 73. [CrossRef]
91. Karčiauskas, M.; Rusak, S.; Saez, A. Quintessential inflation and nonlinear effects of the tachyonic trap mechanism. *Phys. Rev. D* **2022**, *105*, 043535. [CrossRef]
92. Bettoni, D.; Rubio, J. Quintessential Inflation: A Tale of Emergent and Broken Symmetries. *Galaxies* **2022**, *10*, 22. [CrossRef]
93. Fujikura, K.; Hashiba, S.; Yokoyama, J. Generation of neutrino dark matter, baryon asymmetry, and radiation after quintessential inflation. *Phys. Rev. D* **2023**, *107*, 063537. [CrossRef]
94. Dimopoulos, K.; Karam, A.; Sánchez López, S.; Tomberg, E. Palatini R^2 quintessential inflation. *JCAP* **2022**, *10*, 076. [CrossRef]
95. Inagaki, T.; Taniguchi, M. Quintessential Inflation in Logarithmic Cartan $F(R)$ Gravity. *arXiv* **2023**, arXiv:2312.11776.
96. Alho, A.; Uggla, C. Quintessential α-attractor inflation: A dynamical systems analysis. *JCAP* **2023**, *11*, 083. [CrossRef]
97. Giarè, W.; Di Valentino, E.; Linder, E.V.; Specogna, E. Testing α-attractor quintessential inflation against CMB and low-redshift data. *arXiv* **2024**, arXiv:2402.01560.
98. Kofman, L.; Linde, A.D.; Starobinsky, A.A. Reheating after inflation. *Phys. Rev. Lett.* **1994**, *73*, 3195–3198. [CrossRef] [PubMed]
99. Kofman, L.; Linde, A.D.; Starobinsky, A.A. Towards the theory of reheating after inflation. *Phys. Rev. D* **1997**, *56*, 3258–3295. [CrossRef]
100. Greene, P.B.; Kofman, L.; Linde, A.D.; Starobinsky, A.A. Structure of resonance in preheating after inflation. *Phys. Rev. D* **1997**, *56*, 6175–6192. [CrossRef]
101. Felder, G.N.; Kofman, L.; Linde, A.D. Instant preheating. *Phys. Rev. D* **1999**, *59*, 123523. [CrossRef]
102. Parker, L. Particle creation in expanding universes. *Phys. Rev. Lett.* **1968**, *21*, 562–564. [CrossRef]
103. Zeldovich, Y.B.; Starobinsky, A.A. Particle production and vacuum polarization in an anisotropic gravitational field. *Zh. Eksp. Teor. Fiz.* **1971**, *61*, 2161–2175.
104. Grib, A.A.; Mamayev, S.G.; Mostepanenko, V.M. *Vacuum Quantum Effects in Strong Fields*; Friedmann Laboratory Publishing: St. Petersburg, Russia, 1994.
105. Haro, J. Gravitational particle production: A mathematical treatment. *J. Phys. A* **2011**, *44*, 205401. [CrossRef]
106. Khlopov, M.Y.; Linde, A.D. Is It Easy to Save the Gravitino? *Phys. Lett. B* **1984**, *138*, 265–268. [CrossRef]
107. Ellis, J.R.; Kim, J.E.; Nanopoulos, D.V. Cosmological Gravitino Regeneration and Decay. *Phys. Lett. B* **1984**, *145*, 181–186. [CrossRef]
108. Aghanim, N.; Akrami, Y.; Ashdown, M.; Aumont, J.; Baccigalupi, C.; Ballardini, M.; Banday, A.J.; Barreiro, R.B.; Bartolo, N.; Basak, S. et al. Planck 2018 results. VI. Cosmological parameters. *Astron. Astrophys.* **2020**, *641*, A6; Erratum in *Astron. Astrophys.* **2021**, *652*, C4. [CrossRef]
109. Riess, A.G.; Yuan, W.; Macri, L.M.; Scolnic, D.; Brout, D.; Casertano, S.; Jones, D.O.; Murakami, Y.; Anand, G.S.; Breuval, L.; et al. A Comprehensive Measurement of the Local Value of the Hubble Constant with 1 km s^{-1} Mpc^{-1} Uncertainty from the Hubble Space Telescope and the SH0ES Team. *Astrophys. J. Lett.* **2022**, *934*, L7. [CrossRef]
110. Di Valentino, E.; Mena, O.; Pan, S.; Visinelli, L.; Yang, W.; Melchiorri, A.; Mota, D.F.; Riess, A.G.; Silk, J. In the realm of the Hubble tension—A review of solutions. *Class. Quant. Grav.* **2021**, *38*, 153001. [CrossRef]
111. Perivolaropoulos, L.; Skara, F. Challenges for ΛCDM: An update. *New Astron. Rev.* **2022**, *95*, 101659. [CrossRef]
112. Abdalla, E.; Abellán, G.F.; Aboubrahim, A.; Agnello, A.; Akarsu, Ö.; Akrami, Y.; Alestas, G.; Aloni, D.; Amendola, L.; Anchordoqui, L.A. Cosmology intertwined: A review of the particle physics, astrophysics, and cosmology associated with the cosmological tensions and anomalies. *JHEAp* **2022**, *34*, 49–211. [CrossRef]
113. Ivanov, V.R.; Ketov, S.V.; Pozdeeva, E.O.; Vernov, S.Y. Analytic extensions of Starobinsky model of inflation. *JCAP* **2022**, *03*, 058. [CrossRef]
114. Benisty, D.; Guendelman, E.I. Quintessential Inflation from Lorentzian Slow Roll. *Eur. Phys. J. C* **2020**, *80*, 577. [CrossRef]
115. Dimopoulos, K.; Owen, C. Quintessential Inflation with α-attractors. *JCAP* **2017**, *06*, 027. [CrossRef]
116. Felder, G.N.; Kofman, L.; Linde, A.D. Inflation and preheating in NO models. *Phys. Rev. D* **1999**, *60*, 103505. [CrossRef]
117. de Haro, J. Reheating constraints in instant preheating. *Phys. Rev. D* **2023**, *107*, 123511. [CrossRef]

118. de Haro, J.; Aresté Saló, L. Analytic formula to calculate the reheating temperature via gravitational particle production in smooth nonoscillating backgrounds. *Phys. Rev. D* **2023**, *107*, 063542. [CrossRef]
119. Giarè, W.; Pan, S.; Di Valentino, E.; Yang, W.; de Haro, J.; Melchiorri, A. Inflationary potential as seen from different angles: Model compatibility from multiple CMB missions. *JCAP* **2023**, *9*, 019. [CrossRef]
120. Poulin, V.; Smith, T.L.; Karwal, T. The Ups and Downs of Early Dark Energy solutions to the Hubble tension: A review of models, hints and constraints circa 2023. *Phys. Dark Univ.* **2023**, *42*, 101348. [CrossRef]
121. Chen, L.; Huang, Q.G.; Wang, K. Distance Priors from Planck Final Release. *JCAP* **2019**, *2*, 028. [CrossRef]
122. Chevallier, M.; Polarski, D. Accelerating universes with scaling dark matter. *Int. J. Mod. Phys. D* **2001**, *10*, 213–224. [CrossRef]
123. Linder, E.V. Exploring the expansion history of the universe. *Phys. Rev. Lett.* **2003**, *90*, 091301. [CrossRef] [PubMed]
124. de Haro, J.; Nojiri, S.; Odintsov, S.D.; Oikonomou, V.K.; Pan, S. Finite-time cosmological singularities and the possible fate of the Universe. *Phys. Rept.* **2023**, *1034*, 1–114. [CrossRef]
125. Montani, G.; De Angelis, M.; Bombacigno, F.; Carlevaro, N. Metric $f(R)$ gravity with dynamical dark energy as a scenario for the Hubble tension . *Mon. Not. Roy. Astron. Soc. Lett.* **2023**, *527*, L156–L161. [CrossRef]
126. Montani, G.; Carlevaro, N.; De Angelis, M. Modified gravity in the presence of matter creation: Scenario for the late Universe . *Entropy* **2024**, *26*, 662. [CrossRef]
127. Poulin, V.; Smith, T. L.; Karwal, T.; Kamionkowski, M. Early Dark Energy Can Resolve The Hubble Tension. *Phys. Rev. Lett.* **2019**, *122*, 221301. [CrossRef]
128. Sakstein, J.; Trodden, M. Early Dark Energy from Massive Neutrinos as a Natural Resolution of the Hubble Tension. *Phys. Rev. Lett.* **2020**, *124*, 161301. [CrossRef]
129. Niedermann, F.; Sloth, M.S. Resolving the Hubble tension with new early dark energy. *Phys. Rev. D* **2020**, *102*, 063527. [CrossRef]
130. Ivanov, M.M.; McDonough, E.; Hill, J.C.; Simonović, M.; Toomey, M.W.; Alexander, S.; Zaldarriaga, M. Constraining Early Dark Energy with Large-Scale Structure. *Phys. Rev. D* **2020**, *102*, 103502. [CrossRef]
131. Kamionkowski, M.; Riess, A.G. The Hubble Tension and Early Dark Energy. *Ann. Rev. Nucl. Part. Sci.* **2023**, **73**, 153–180. [CrossRef]
132. Efstathiou, G.; Rosenberg, E.; Poulin, V. Improved Planck Constraints on Axionlike Early Dark Energy as a Resolution of the Hubble Tension. *Phys. Rev. Lett.* **2024**, *132*, 221002. [CrossRef] [PubMed]
133. Seto, O.; Toda, Y. DESI constraints on the varying electron mass model and axionlike early dark energy. *Phys. Rev. D* **2024**, *110*, 083501. [CrossRef]
134. Jedamzik, K.; Pogosian, L.; Zhao, G.-B. Why reducing the cosmic sound horizon alone can not fully resolve the Hubble tension. *Commun. Phys.* **2021**, *4*, 123. [CrossRef]
135. Vagnozzi, S. Seven Hints That Early-Time New Physics Alone Is Not Sufficient to Solve the Hubble Tension. *Universe* **2023**, *9*, 393. [CrossRef]
136. Riotto, A. Inflation and the theory of cosmological perturbations. *ICTP Lect. Notes Ser.* **2003**, *14*, 317–413